Entropy Barriers to Proton Transfer

Michael Meot-Ner (Mautner)*,† and Sean C. Smith‡

Contribution from the Chemical Kinetics Division, National Institute of Standards and Technology, Gaithersburg, Maryland 20899, and Department of Chemistry, University of Canterbury, Christchurch 1, New Zealand. *Received May 8, 1989*

Abstract: Proton transfer between sterically hindered pyridines and amines proceeds through locked-rotor, low-entropy intermediates. The reactions exhibit slow kinetics (efficiencies of 0.1–0.0001) and large negative temperature coefficients (up to $k = CT^{-8.7}$). The rates become slower and the temperature dependencies steeper with increasing steric hindrance. The observations are reproduced by a multiple complex-switching RRKM model that allows several alternative complexes to be rate controlling: a series of loose complexes, a locked-rotor tight complex that occurs before the formation of a hydrogen-bonded complex, and a complex located at the central barrier. The rate-limiting transition state shifts from the loose to the tight and central-barrier complexes with increasing temperature. The model suggests that at elevated temperatures, above 1000 K, ion–molecule reactions will become slow even for unhindered, small reactants. Ion kinetics may then become similar to neutral radical kinetics.

Introduction

Interesting kinetics were observed in hydride-transfer reactions involving branched hydrocarbons and carbonium ions. The kinetics showed slow rates and uniquely large negative temperature coefficients,[1-3] up to $k = CT^{-6}$. The rates decreased and the temperature coefficients became larger with increasing steric hindrance about the reaction centers. Some slow proton-transfer reactions involving alkylbenzenes also showed large negative temperature coefficients, up to $k = CT^{-7}$.[4,5]

Slow kinetics in hindered systems result because, in a large fraction of the collisions, steric effects prevent close approach of the reactive centers. With increasing temperature, the formation of the tight intermediate required for the reaction becomes increasingly less likely. In the present paper, we shall use alkylpyridines to demonstrate clearly the linkage of steric hindrance with slow rates and large negative temperature coefficients. Space-filling models of these reactants show that the alkyl rotors must strongly interfere with each other and freeze in order that the reactive nitrogen centers may approach. Indeed, Jasinski and Brauman observed slow kinetics in proton transfer to the strongly hindered 2,6-di-*tert*-butylpyridine.[6]

Transition-state theory (TST) ascribes the slow rates and large negative temperature coefficients observed in hydride-transfer reactions to entropy effects.[1-3] The TST expression for rate constants is $k = k(k_BT/h)\exp(\Delta S^{\ddagger}/R)\exp(-\Delta H^{\ddagger}/RT)$. When m rotors freeze in forming the transition state, the effects on $\Delta S^{\ddagger}$ lead to a temperature coefficient of $T^{-(2+(m/2))}$. This, combined with the enthalpy factor, can lead to substantial negative temperature coefficients. The same effects can be modeled by RRKM calculations.[7]

According to Brauman's double-well model, slow ion–molecule reactions are caused by entropy barriers, i.e., transition states with low densities of states.[8] The sequence of intermediates is summarized in eq 1, and the corresponding potential and free energy surfaces are shown in Figures 1 and 2.

$$AH^+ + B \rightarrow (AH^+\cdot B)^{\ddagger}_{loose} \rightarrow (AH^+\cdot B)^{\ddagger}_{tight}$$

$$(AH^+\cdot B)^{\ddagger}_{HB} \rightarrow (AH\cdot B)^{+\ddagger}_{barrier} \rightarrow BH^+ + A \qquad (1)$$

The various stages of the reaction in proton transfer between alkylpyridines are illustrated schematically in eq 2.

Strong steric hindrance in the complexes, denoted $(AH^+\cdot B)_{tight}$, $(AH^+\cdot B)^{\ddagger}_{HB}$, and $(AH\cdot B)^{+\ddagger}_{barrier}$, is indicated by space-filling models and by the large negative entropies (up to −50 cal/(mol K)) for the formation of hydrogen-bonded complexes of hindered pyridines.[9]

We shall investigate proton transfer in sterically hindered systems experimentally, followed by RRKM models that consider

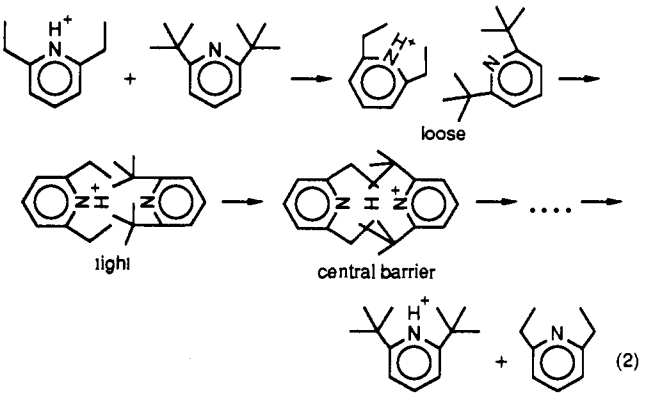

(2)

the effects of several possible rate-limiting transition states along the reaction path.

Experimental Section

The measurements were done with the NIST pulsed high-pressure mass spectrometer.[10] Reaction mixtures of 0.1–0.001% amine or alkylpyridine reactants in cyclohexane or methanol vapor were prepared in a bulb heated to 180 °C and allowed to flow to the ion source in a stainless steel line heated to 150 °C. The reaction mixture was ionized by 0.5–1-ms pulses of 500–1000-eV electrons, and relative ion signal intensities of reactant and product ions followed for 0.5–2 ms after the pulse.

The reactants that were purchased from commercial sources had nominal purities of >98% and were used as purchased.

Results

1. Rate Constants in Hindered Pyridines. Rate constants were calculated from the variation of relative ion intensities with reaction time. Some of the reactions proceeded to completion, and irreversible kinetics applied. In several reactions, where the difference between the proton affinities of the reactants was less than ≈4 kcal/mol, equilibrium was achieved and reversible kinetics were applied.

† National Institute of Standards and Technology.
‡ University of Canterbury.

(1) Solomon, J. J.; Meot-Ner (Mautner), M.; Field, F. H. *J. Am. Chem. Soc.* **1974**, *96*, 3727.
(2) Meot-Ner (Mautner), M.; Solomon, J. J.; Field, F. H.; Gershinowitz, H. *J. Phys. Chem.* **1974**, *78*, 1733.
(3) Meot-Ner, M.; Field, F. H. *J. Chem. Phys.* **1976**, *64*, 277.
(4) Stone, J. A. In *Structure/Reactivity and Thermochemistry of Ions*, Ausloos, P., Lias, S. G., Eds.; Reidel: Dordrecht, 1987; p 391.
(5) Li, X.; Stone, J. A. *Can. J. Chem.* **1987**, *65*, 2454.
(6) Jasinski, J. M.; Brauman, J. I. *J. Am. Chem. Soc.* **1980**, *102*, 2906.
(7) Magnera, T. F.; Kebarle, P. In *Ionic Processes in the Gas Phase*; Almoster-Ferreira, M. A., Ed.; Reidel: Dordrecht, 1984; p 135. Sunner, J. A.; Hirao, K.; Kebarle, P. *J. Phys. Chem.* **1989**, *93*, 4010.
(8) Olmstead, W. N.; Brauman, J. I. *J. Am. Chem. Soc.* **1979**, *101*, 3715.
(9) Meot-Ner (Mautner), M.; Sieck, L. W. *J. Am. Chem. Soc.* **1983**, *105*, 2956.
(10) Sieck, L. W.; Meot-Ner (Mautner), M. *J. Phys. Chem.* **1984**, *88*, 5324.

0002-7863/91/1513-862$02.50/0

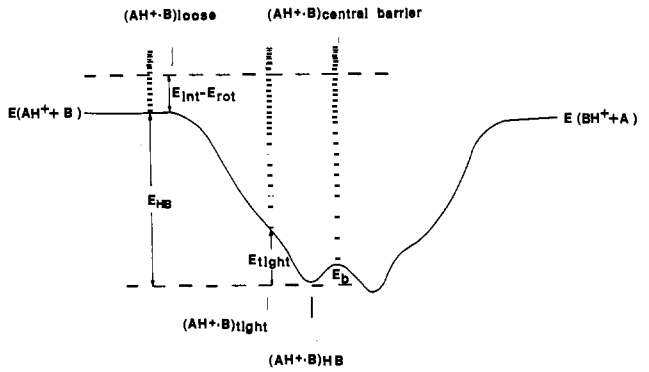

Figure 1. Schematic potential energy surface for bimolecular ion–molecule reactions.

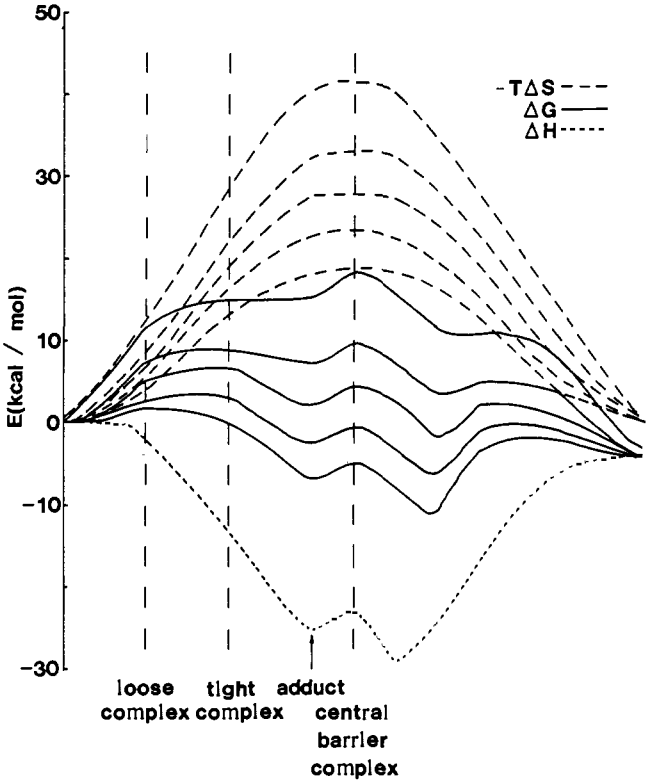

Figure 2. Enthalpy, entropy (i.e., $-T\Delta S$), and free energy surfaces for a model of the proton-transfer reaction from 2,6-Et_2PyrH$^+$ to 2,6-*t*-Bu_2Pyr. For $-T\Delta S$ to ΔG the curves from bottom to top correspond to 400–800 K in 100 K increments. Note that the maximum free energy shifts from the loose to the tight and central complex with increasing temperature.

We checked that the measured rate constants were independent of mixture composition by varying the concentrations by up to a factor of 10. The rate constants were also independent of the total pressure in the usable range of 0.3–2 Torr. From such checks and replicate measurements, the error is estimated as ±30%.

Below ≈180 °C, cluster ions were present in significant concentrations and this prohibited straightforward kinetic measurements. Nevertheless, rate constants could be obtained from the assumption that the reactant dimer ions, in which the proton is sterically unaccessible, do not transfer a proton or switch ligands. The system is described by eqs 3 and 4, and k_3 is calculated after correcting for equilibrium 4.

$$AH^+ + B \rightarrow BH^+ + A \quad (3)$$

$$AH^+ + A \rightleftarrows A_2H^+ \quad (4)$$

$$A_2H^+ + B \rightarrow BH^+ + 2A \quad (5)$$

$$A_2H^+ + B \rightarrow BH^+\cdot A + A \quad (6)$$

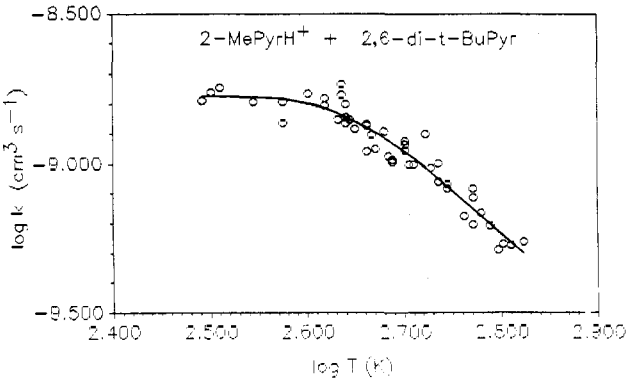

Figure 3. Temperature dependence of proton transfer from 2-MePyrH$^+$ to 2,6-*t*-Bu_2Pyr. The line is fourth-order regression through experimental points. Rate constants below 440 K (log T = 2.64) were corrected for clustering equilibria and below 380 K (log T = 2.58) according to the parallel reaction kinetics described in the text.

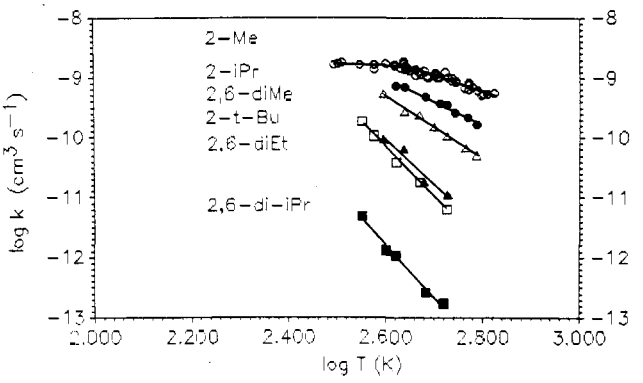

Figure 4. Temperature dependence of proton transfer from the protonated ions of the compounds shown to 2,6-*t*-Bu_2Pyr. Rate constants below 440 K (log T = 2.64) were corrected for clustering equilibria.

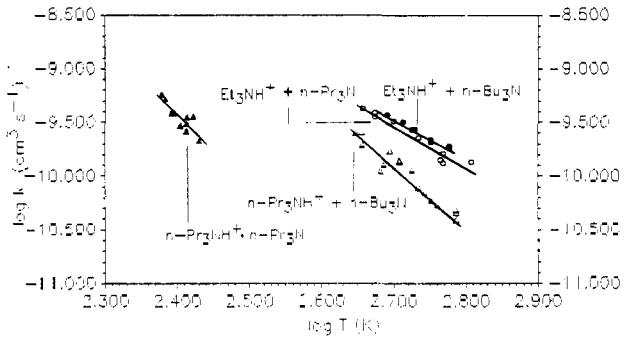

Figure 5. Temperature dependence of proton transfer between alkylamines. The line labeled *n*-Pr_3NH^+·*n*-Pr_3N shows rate constants for the clustering reaction.

A different situation arises at lower temperatures, where the cluster-forming raction (4) is irreversible. Under these conditions, reactions 3 and 4 constitute parallel reactions and the total rate constant as obtained from the decay of AH$^+$ can be proportioned to k_1 and k_2 according to the ratio of the products BH$^+$ and A_2H^+. These treatments were applied to some of the data in Figures 3–5 as indicated in the figure captions.

The temperature dependencies of slow ion–molecule reactions may be best expressed, both on the basis of TST and empirical considerations, in the form $k = CT^n$, and often linear plots of log k vs log T are found.[1-3] Such plots are shown for the present reactions in Figures 3–5. The results are summarized in Table I.

The results show correlations of the degree of alkyl substitution with decreasing rate constants and increasingly negative temperature coefficients. The magnitude of the coefficient observed in the most strongly hindered system, the cation of 2,6-*i*-Pr_2Pyr

Table I. Kinetics and Thermochemistry of Proton-Transfer Reactions $AH^+ + B \rightarrow BH^+ + A$

AH^+	$-\Delta H°$ [a]	k_{450} [b]	k_{600} [b]	n [b]	log C [b]	T_{tr} (K) [b]
		Pyridines, B = 2,6-i-Pr_2Pyr				
2-t-BuPyrH$^+$	4.6[c]	8.6				
2,6-Et_2PyrH$^+$	1.7[d]	10.6				
		Pyridines, B = 2,6-t-Bu_2Pyr				
2-MePyrH$^+$	8.4	13.0	5.3	−3.1	−0.66	454
2-i-PrPyrH$^+$	6.2	7.9	2.6	−3.8	0.98	375
2,6-Me_2PyrH$^+$	4.8[e]	2.4	0.52	−5.3	4.44	315
2-t-BuPyrH$^+$	4.1[f]	0.40	0.046	−7.5	9.50	275
2,6-Et_2PyrH$^+$	2.3	0.20	0.018	−8.3	11.32	266
2,6-i-Pr_2PyrH$^+$	1.2[g]	0.0057	0.00047	−8.7	10.84	181
		Amines, B = n-Pr_3N				
Et_3NH^+	3.0[h]	4.0	1.3	−3.8	0.68	312
		Amines, B = n-Bu_3N				
Et_3NH^+	5.4[i]	4.8	1.7	−3.6	0.23	322
n-Pr_3NH^+	2.9[j]	1.1	0.64	−5.4	4.81	331

[a] Units of kcal/mol. Values from ref 27 or from the present results as noted below. [b] k in units of 10^{-10} cm^3 s^{-1}. n and log C for temperature coefficients in $k = CT^{-n}$ obtained from linear regression of plots in Figures 4 and 5. T_{tr} (K) is temperature where extrapolated plots reach $k_{coll} \approx 1.5 \times 10^{-9}$ cm^3 s^{-1}. [c-g] From $\Delta G°$ values at one temperature and assuming $\Delta S° = 0$. Temperatures of measurement (K): *c*, 485; *d*, 525; *e*, 480; *f*, 397; *g*, 357. [h] From temperature study, $\Delta H° = -3.0$ kcal/mol, $\Delta S° = -0.4$ cal/(mol K). [i] From $\Delta G°$ (602) = −4.2 kcal/mol, assuming $\Delta S° = -2$ cal/(mol K) similar to reaction in *j*. [j] From temperature study, $\Delta H° = -2.9$ kcal/mol, $\Delta S° = -2.1$ cal/(mol K).

+ 2,6-t-Bu_2Pyr, where $k = CT^{-8.6}$, is the largest negative temperature coefficient reported so far for any bimolecular chemical reaction.

2. Proton Transfer in Large Alkylamines. Unlike in the hindered pyridines, the substituents even in large alkylamine systems such as $(n\text{-}C_3H_7)_3NH^+ + (n\text{-}C_4H_9)_3N$ can be oriented so that they do not interfere directly with the reaction center. The negative entropy effect in the complexes arises since the alkyl groups in the two reactants decrease the free volume available for internal rotations. In this respect, the steric hindrance is similar to hydride transfer in branched hydrocarbons.

Table I and Figure 5 show proton transfer between tertiary amines, with slow kinetics and significant negative temperature coefficients similar to those observed in alkylpyridines. We note that the thermochemistry of the hindered amine complexes is also similar to those of hindered pyridines.[9]

3. Relation between Proton Transfer and Association Kinetics. The slow proton-transfer rates show that a large fraction of the complexes formed by capture collisions cannot reach the optimized hydrogen-bonded conformation that is needed for proton transfer. A similar effect may also prevent the formation of stabilized A_2H^+ dimers. The mechanism is shown in eq 7.

$$AH^+ + A \rightarrow (AH^+\cdot A)^*_{loose} \rightarrow (AH^+\cdot A)^*_{tight} \rightarrow (AH^+\cdot A)^*_{HB} \xrightarrow{M} (AH^+\cdot A)_{HB} \quad (7)$$

The mechanism is analogous to proton transfer in eq 1. Reflection from $(AH^+\cdot A)^*_{tight}$ may prevent the formation of the hydrogen-bonded complexes in most collisions. However, those excited complexes that do form will all be stabilized at sufficiently high pressures, and pseudo-second-order high-pressure kinetics will be reached with a rate constant $k_{assoc}^{(2)}$. The reaction efficiency $k_{assoc}^{(2)}/k_{coll}$ then reflects the fraction of collisions leading to $(AH^+\cdot A)^*_{HB}$. This should be comparable to the efficiency k_{pt}/k_{coll}, (pt = proton transfer) which reflects the fraction of collisions leading to $(AH^+\cdot B)^*$ in similarly hindered proton-transfer systems. In both cases, the overall second-order rate constants may be substantially smaller than the collision rate.[11]

We measured rate constants for reaction 7 with A = n-Pr_3N. Pressure studies in the 1–2-Torr range showed kinetics at or near the high-pressure limit. Consistent with eq 7, the pseudo-second-order rates are below the collision rate and exhibit negative temperature coefficients comparable to the proton-transfer reactions (Figure 5). However, these rates are slower than those expected for k_{Pt}, which would be at k_{coll} at the same temperatures (Figure 5). Further studies comparing proton transfer and association kinetics would be of interest.

RRKM Models. The various complexes and transition states to be considered are indicated in Figure 1.

Slow ion–molecule reactions are usually interpreted by the double-well model first developed by Brauman and co-workers.[8] That model assumes a low density of states, i.e., low entropy at the barrier separating the two energy wells (Figure 1). This is the rate-limiting transition state. On the other hand, in the model of Magnera and Kebarle for hydride transfer, the rate-limiting transition state is the loose complex at low temperatures, switching to the locked-rotor tight complex at high temperatures.[7] Similar to the case of double-well model, the latter is also a low-entropy rate-limiting transition state, but at a position preceding an optimized strongly bonded adduct on the potential energy surface (Figure 1). This approach reproduced the experimental temperature dependence, including the observed transition from collision-limited to slow kinetics. Complex-switching models were also used by other authors.[12-16]

In a model that unifies the two approaches, we consider any of the loose, tight, and central-barrier complexes as potentially rate limiting. The kinetics corresponds to eqs 8 and 9.

$$AH^+ + B \underset{k_b}{\overset{k_{cap}}{\rightleftharpoons}} (AH^+\cdot B)^*_{HB} \xrightarrow{k_p} BH^+ + A \quad (8)$$

$$k_f = k_{cap}\frac{k_p}{k_b + k_p} \quad (9)$$

The overall rate k_f may be limited by the capture rate k_{cap}, which corresponds to the formation of $(AH^+\cdot B)^*_{HB}$ through the loose and tight complexes, and may be much smaller than k_{coll} if the tight complex is limiting, or by k_p, which is the rate of dissociation to products through the central barrier. The former case corresponds to the complex-switching, locked-rotor model; the latter corresponds to the double-well model. Therefore, the present approach can accommodate either model and allows the RRKM calculations of k_{cap}, k_b, and k_p to identify the appropriate rate-limiting complex.

RRKM parameters for the various complexes are described in detail in Appendix II. The energies of the complexes are estimated from the thermochemistry of protonated alkylpyridine dimers. Frequencies of the pyridine moieties and alkyl substituents are

(11) Meot-Ner (Mautner), M. In *Ion–Molecule Reactions*; Bowers, M. T., Ed.; Academic Press: New York, 1979; Vol. 1, p 198.

(12) Dodd, J. A.; Golden, D. M.; Brauman, J. I. *J. Chem. Phys.* **1984**, *80*, 1894.

(13) Truhlar, D. G. *J. Chem. Phys.* **1985**, *82*, 2166.

(14) Chesnavich, W. J.; Bowers, M. T. *J. Chem. Phys.* **1985**, *82*, 2168.

(15) Dodd, J. A.; Golden, D. M.; Brauman, J. I. *J. Chem. Phys.* **1985**, *82*, 2169.

(16) Chesnavich, W. J.; Bass, L.; Su, T.; Bowers, M. T. *J. Chem. Phys.* **1981**, *74*, 2228.

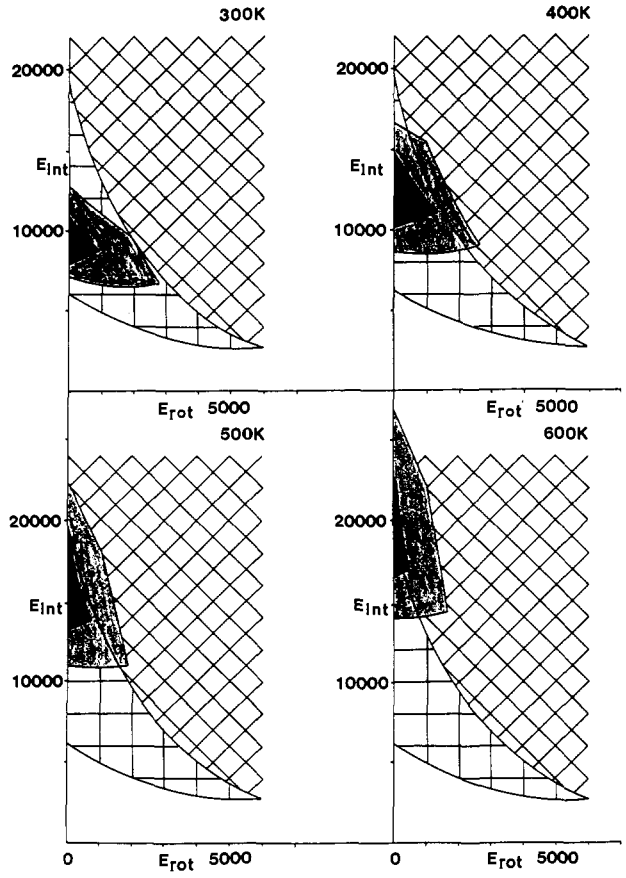

Figure 6. Relation between the rate-controlling entity and the reactant flux at various temperatures. The gridded area corresponds to E_{int} and E_{rot} values (cm^{-1}) where the loose complex is rate limiting, and the cross-hatched area corresponds to the values where the tight complex is rate limiting. The heavily shaded area contains flux values over 50% and the lightly shaded areas contain over 10% of the maximum microscopic flux. With increasing temperature, the flux shifts to the high-energy area where the tight complex is rate limiting.

assigned by use of spectroscopic data.

All of the vibrations in the complexes that are formed by the freezing of rotors are assigned a common frequency ν_{tight}, which affects the densities of states and the entropies of the complexes. The values of ν_{tight} (and similarly ν_b for the central-barrier complex) and the energy of the tight complex E_{tight} are adjustable parameters.

The microcanonical multiple-complex RRKM program[17,18] is used as follows. We calculate the microscopic unimolecular dissociation rates $k_b(E_{int}, E_{rot})$ of the chemically activated hydrogen-bonded complex $(AH^+ \cdot B)_{HB}^*$ through transition states corresponding to $(AH^+ \cdot B)_{tight}$ and $(AH^+ \cdot B)_{loose}$ (Figure 1). The program identifies whether the minimum flux for each E_{int}, E_{rot} energy level is at the loose or at the tight complex. The minimum flux at each E_{int}, E_{rot} is then integrated over the population to calculate the macroscopic k_b. Similarly, the program also calculates $k_p(E_{int}, E_{rot})$ for the dissociation of $(AH^+ \cdot B)_{HB}^*$ to products through the $(AH^+ \cdot B)_b$ transition state at the central barrier. These values are then also integrated to find the macroscopic rate constant k_p.

The macroscopic capture rate k_{cap} is then obtained from $k_{cap}/k_b = K$, where K is the equilibrium constant to form the hydrogen-bonded complex $(AH^+ \cdot B)$, as obtained from estimated thermochemistry. Note that the macroscopic k_{cap} at any temperature is a composite value of microscopic rates $k_b(E_{int}, E_{rot})$, some of which (at low E_{int} and E_{rot}) correspond to loose-complex-limited fast kinetics and some (at high E_{int} and E_{rot}) to tight-complex-limited slow kinetics.

(17) Smith, S. G.; McEwan, M. J.; Gilbert, R. G. *J. Chem. Phys.* **1989**, *90*, 1630.

(18) Smith, S. C.; Gilbert, R. G. School of Chemistry, University of Sidney, N.S.W. 2006, Australia (available on request).

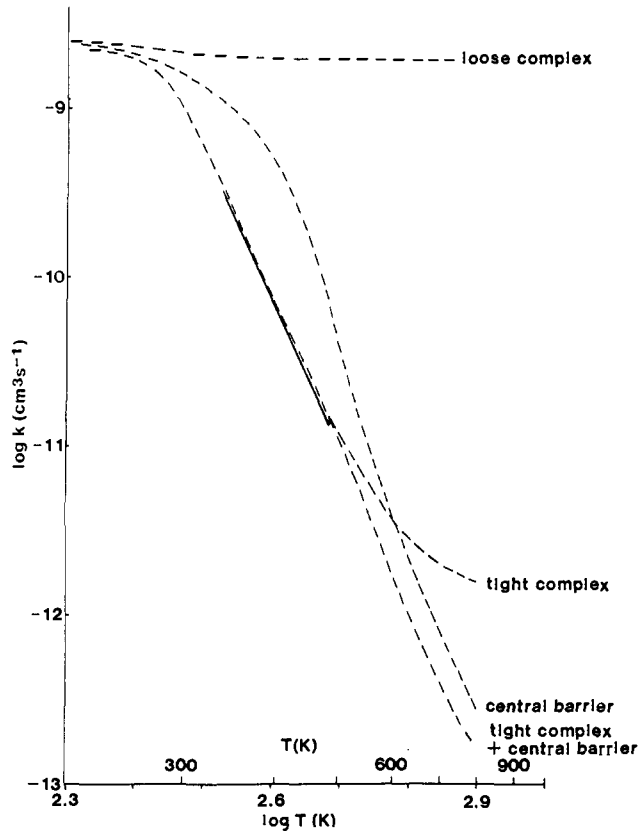

Figure 7. Temperature dependence of calculated proton-transfer rate constant from the cation of 2,6-diethylpyridine to 2,6-di-*tert*-butylpyridine. The adjustable parameters are E_{tight} = 12.0 kcal/mol, ν_{tight} = 80 cm^{-1} and E_b = 2.0 kcal/mol, ν_b = 140 cm^{-1}. The solid line shows the experimental temperature dependence. In all the calculations, the loose complex plus the complexes indicated are present.

Mechanism of Complex Switching. The underlying reason for switching from loose- to tight-complex-limited kinetics is illustrated in Figure 6. The figure shows the energy ranges of E_{int} and E_{rot} at which the loose complex or the tight complex is rate limiting. On this map are superimposed the population distributions (shaded areas) at various temperatures. At high temperatures, more population shifts into the region limited by the tight complex and the behavior shifts from collision-limited fast kinetics to slow kinetics. This is the RRKM mechanism for transition from fast to slow kinetics as observed both experimentally (Figure 3) and theoretically (Figures 7 and 8).

The thermochemical reason for complex switching is illustrated in Figure 2. This shows the transition from the loose-complex-dominated free energy barrier at 400 K to the tight-complex-dominated free energy barrier at 600 K.

In summary, in our original TST arguments,[1-3] as well as the present RRKM and thermochemical models and the Magnera–Kebarle model,[7] the switching from loose-complex-limited fast kinetics to tight-complex-limited slow kinetics arises because of the entropy effects of locked rotors at high temperatures.

Kinetic Effects of the Various Complexes. The rate constant as it would be determined by each of the loose, tight, and central-barrier complexes alone and all combined is illustrated in Figure 7. The figure shows that the loose complex alone, without other rate-limiting entities, would give proton transfer at the ion–molecule collision rate at all temperatures. When the tight complex is added, the rate is still close to the collision rate at low temperatures, but above 300 K it gives slower rates and large negative temperature coefficients that start to level off above 500 K. In the model with all three complexes, above 600 K, the central complex becomes rate limiting. The combined effect of the multicomplex model with eq 9 gives a fairly sharp transition from

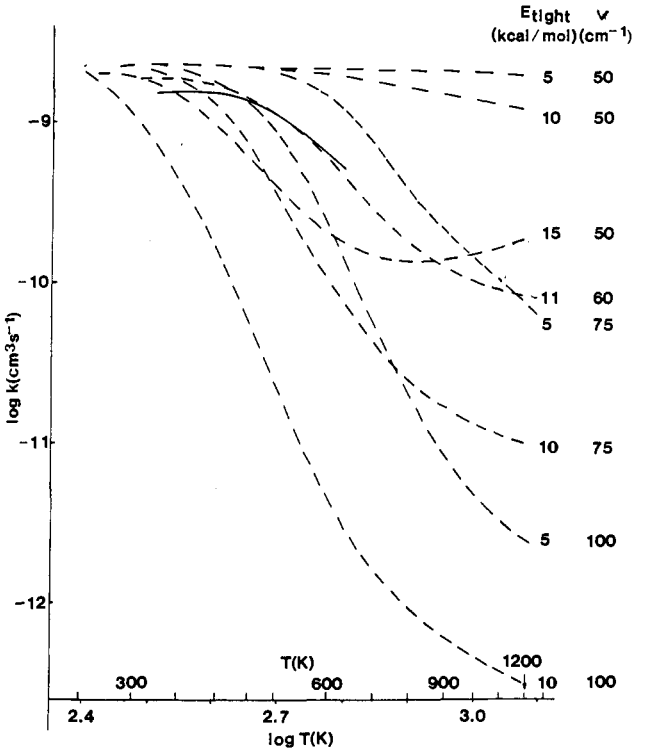

Figure 8. Kinetic effects of the tight complex with various adjustable parameters E_{tight} (kcal/mol) and ν_{tight} (cm^{-1}) as shown. Results are for a model for 2-$MePyrH^+$ + 2,6-t-Bu_2Pyr, including the loose and tight complexes but without the central barrier. The solid line shows the experimental temperature dependence.

fast to slow kinetics at 300 K and a large negative temperature coefficient of the form $\log k = a - b \log T$ over a wide temperature range, 300–800 K.

Best agreement with experiment for the 2,6-Et_2PyrH^+ + 2,6-t-Bu_2Pyr is achieved by the tight-complex-limited model. On the other hand, the central-complex-limited model with any reasonable values of E_{HB} and ν_b could not reproduce the experimental results.

Space-filling models show that in the rate-controlling tight complex the steric interference of the alkyl groups is nearly fully developed (a large $-T\Delta S^{\ddagger}$ term), but the NH^+–N separation is far too large for efficient bonding (a small $\Delta H^{\ddagger}$ term). This combination yields a free energy barrier.

The effects of the adjustable parameters E_{tight} and ν_{tight} are illustrated in Figure 8. The absolute values of the rate constants decrease with increasing E_{tight}, as the free energy barrier at the tight complex increases. On the other hand, the temperature coefficients are affected primarily by ν_{tight}, i.e., densities of states. The rate constants decrease and the negative temperature coefficients become larger as ν_{tight} increases, i.e., with increasing hindrance. In TST terms, the temperature coefficients are affected primarily by $\Delta S^{\ddagger}$ rather than $\Delta H^{\ddagger}$.

Figure 8 also shows the experimental plot for 2-$MePyrH^+$ + 2,6-t-Bu_2Pyr, which changes from fast to slow kinetics. This is well-matched by the tight complex with E_{tight} = 11 kcal/mol (corresponding to an interaction energy of 14 kcal/mol between the reactants) and with ν_{tight} = 60 cm^{-1} (which corresponds to $\Delta S°_{tight}$ = −36 cal/(mol K)). These values are consistent with the thermochemical estimates (Appendix II). We also found that the experimental transition from slow to fast kinetics cannot be reproduced by central-complex-limited kinetics by use of any reasonable values of E_{HB} and ν_b.

In summary, the entropy effects of frozen rotors in the tight complex are the primary kinetic factor in the observed temperature range. The tight complex, rather than the central-barrier complex, is identified as the rate-limiting entity under the experimental conditions.

An interesting feature of the results is that the calculated rate constants do not continue to decrease indefinitely with increasing temperature. Figure 8 shows that the rate constants tend to level off and even reverse at high temperatures.

A qualitative reason is that at high temperatures the partition functions of the torsions in the tight complex can approach and even surpass the partition functions of the rotors from which they are formed. For example, the partition functions of a 120-cm^{-1} torsion and a one-dimensional methyl rotor (B = 3.62 cm^{-1}) are, respectively, 2.3 and 4.5 at 300 K; 6.3 and 8.2 at 1000 K; and 12.1 and 11.6 at 2000 K.

The leveling-off effect may not be reflected in the overall rate constant k_f, which can continue to decrease because the even tighter complex at the central barrier becomes rate controlling (Figure 7). Ultimately, however, the rate constants due to the central adduct should also level off. An example is observed in Figure 9.

Temperature Effects in Unhindered Reactants. Even in unhindered reactants, molecular rotations can become hindered as the reactants approach.[12-16] This was discussed by Dodd et al.,[12]

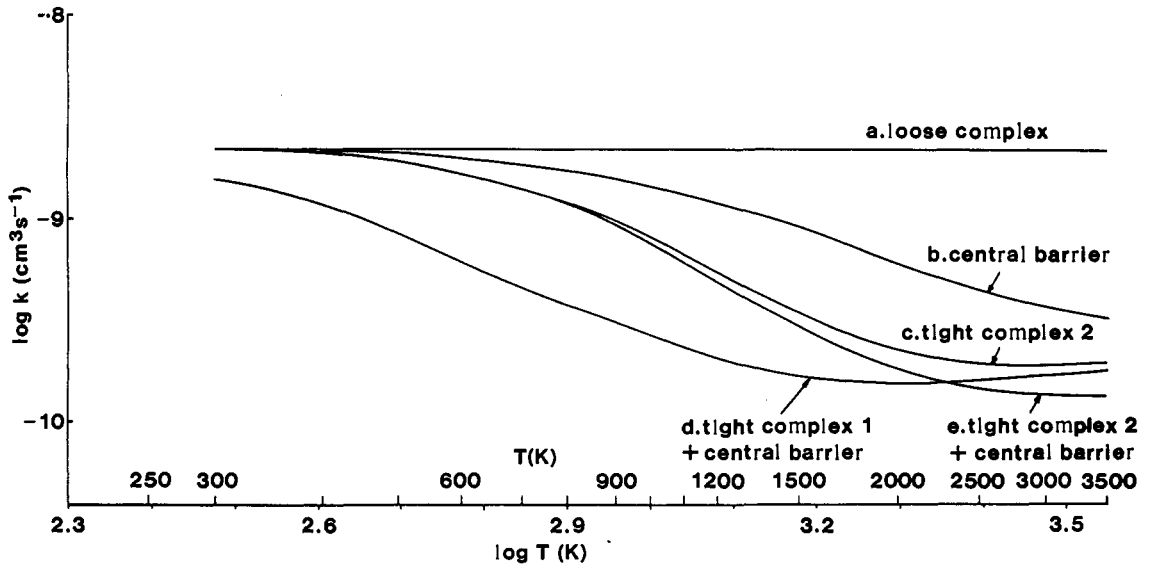

Figure 9. Temperature dependence of calculated proton-transfer rate constant from NH_4^+ to CH_3NH_2: (a) loose complex only; (b) loose complex plus a central barrier with E_b = 2 kcal/mol, ν_b = 250 cm^{-1}; (c) loose complex plus tight complex with E_{tight} = 10 kcal/mol, ν_{tight} = 200 cm^{-1}; (d) loose complex plus tight complex with E_{tight} = 15 kcal/mol, ν_{tight} = 150 cm^{-1}, plus central barrier with E_b = 2 kcal/mol, ν_b = 250 cm^{-1}; (e) loose complex plus tight complex with E_{tight} = 10 kcal/mol, ν_{tight} = 200 cm^{-1}, plus central barrier with E_b = 2 kcal/mol, ν_b = 250 cm^{-1}.

Truhlar,[13] and Chesnavich and Bowers.[14] The possible effects at high energies were noted, but no specific calculations of the temperature effects were given.

We construct a model for the smallest reactants for exothermic proton transfer in amines, $NH_4^+ + CH_3NH_3$. The rates are calculated up to 3500 K to demonstrate the general predictions of the model for unhindered reactants, although these particular reactants may pyrolize at these temperatures. A detailed description of the model is given in Appendix II.

As above, the parameters ν_{tight} (here for torsions formed from molecular rotations) and the energy of the tight complex E_{tight} are adjustable parameters. We use two sets of parameters. Complex 1 is a weakly bonded tight complex, with an $NH_4^+ \cdot CH_3NH_2$ interaction energy of 6 kcal/mol (corresponding to E_{tight} = 15 kcal/mol) and ν_{tight} = 150 cm^{-1}. Complex 2 is tighter, with $NH_4^+ \cdot CH_3NH_2$ interaction energy of 11 kcal/mol (corresponding to E_{tight} = 10 kcal/mol) and ν_{tight} = 200 cm^{-1}.

The results are shown in Figure 9. The parameters for the weaker tight complex 1 lead to fall-off from the collision rate already at 500–600 K, which is unreasonable because exothermic proton-transfer reactions usually proceed at collision rates at these temperatures. The parameters of the more strongly interacting complex 2 lead to transition to slow kinetics at about 1000 K. This may be a more realistic behavior.

Figure 9 shows the effects of the tight complex (complex 2) alone, the central barrier alone, and the full multiple-complex model. Here the effects of the tight complex alone or in combination with the central-barrier complex are comparable, since the frequencies ν_{tight} and ν_b are similar (200 or 250 cm^{-1}, respectively). Although the energies of the complexes differ by 8 kcal/mol, this becomes insignificant at high temperatures.

The calculated proton-transfer rate decreases and then levels off above about 2000 K. The reasons are similar to the high-temperature leveling off of the rate in the pyridines.

The calculations demonstrate that rotational constraints even with simple reactants[12-16] can yield slow rates at very high temperatures.

Conclusions

Proton transfer in hindered pyridines constitutes a clear example of tight complexes with locked rotors. With increasing temperature, the kinetics exhibit transition from fast to slow kinetics and large negative temperature coefficients are observed, up to $k = CT^{-8.6}$.

The known thermochemistry of related adducts constrains the parameters of the rate-limiting complexes. The observed kinetic features are reproduced best with parameters that can be attributed to the tight complex rather than the complex at the central barrier.

The roles of the loose and tight complexes here are similar to those suggested by Magnera and Kebarle for hydride-transfer reactions.[7] However, our model suggests in addition that the rate-limiting entity will shift continuously inward (toward the right on Figure 1) with increasing temperature, through a succession of loose complexes, tight complexes, and finally the central barrier. This multiple-complex-switching model reproduces well the observed fairly sharp transition from fast to slow kinetics and also gives a linear log k vs log T plot over a wide temperature range. The calculations also suggest that the negative temperature coefficients may level off and even reverse at very high temperatures.

The present models that consider only one tight complex are semiquantitative. In fact, the transition state should shift inward through a succession of increasingly energetically stabilized but constrained tight complexes.

In analogy with the observed kinetics in hindered systems, ion–molecule reactions with unhindered reactants can also experience some rotational constraints at close approach of the reactants. In the hindered systems, the $-T\Delta S^\ddagger$ term is large enough to bring slow kinetics into the observable 300–500 K range. By analogy, in unhindered systems, similar but smaller entropy effects can lead to slow kinetics at higher temperatures. The resulting slow rates, negative temperature coefficients, and high-temperature leveling-off effects may be important for ion–molecule reactions in flames and plasmas.

With increasing temperature, the rate-limiting transition state shifts to smaller reactant separations, toward complexes with increasingly lower energies but also lower entropies, as the $-T\Delta S^\ddagger$ term increases. Ultimately, ion–molecule transition states will involve separations as small as in neutral–neutral radical reactions. Interestingly, therefore, at high temperatures ion–molecule kinetics may become similar to neutral radical kinetics.

Acknowledgment. This work was supported in part by the Office of Basic Energy Sciences, U.S. Department of Energy. The support of the University Grants Committee Postgraduate Scholarship and Shirtcliffe Fellowship for S.C.S. is gratefully acknowledged. We thank Dr. Murray McEwan for helpful discussions.

Appendix I

Microcanonical Variational Multiple-Complex-Switching RRKM Model. In applying microcanonical variational transition-state theory to the proton-transfer reactions, we calculate the microscopic rate coefficient $k(E,J)$ by the well-known RRKM formula A1.

$$k(E,J) = \frac{W_{min}^\ddagger(E - V_{eff}(s))}{h\rho(E - R)} \tag{A1}$$

where

$$W_{min}^+(E - V_{eff}(s)) = \int d\epsilon_+ \, \rho^+(\epsilon_+) \tag{A2}$$

In eq A1, $V_{eff}(s)$ is the effective potential at the position $r = s$ of the transition state: $V_{eff}(s) = V(s) + (I/I^+)R$ where $V(s)$ is the interaction potential, I is the moment of inertia for the external inactive rotation of the collision complex, I^+ is the corresponding moment of inertia for orbital rotation at the transition state, and $R = E_{rot} = BJ(J + 1)$ with $B = h^2/2I$. Then $E - R = E_{int}$ is the energy of the active modes in the collision complex that is available for decomposition.[19] In eq A2, $\rho^+(\epsilon_+)$ is the density of states evaluated at the position $r = s$ of the transition state (excluding the reaction coordinate degree of freedom). The value of s is chosen so as to minimize the sum of states $W^+(E - V_{eff}(r))$ and hence to locate the "bottleneck" in phase space for the particular combination of E and J.[20] The rotational-state counting allows correct incorporation of the effect of the hindered dipole rotation in the loose transition state on the sum of states. Variational treatment applies to the different complexes in the capture channel. In addition, the rate of decomposition competitively in a second channel, corresponding to the forward reaction through the central barrier, is also calculated, and these results yield the ratio of forward to reverse decomposition.[8]

Capture rates k_{cap} are obtained by first thermally averaging $k(E,J)$ according to A3 to obtain the equilibrium, high-pressure-limiting rate coefficient. The rate of capture from reactants is then obtained from eqs A4 and A5.

$$k^\infty_{uni} = \int_0^\infty dJ \, (2J + 1) \int_{E_0(J)}^\infty d\epsilon_{int} \, k(\epsilon_{int},J) \frac{\rho(\epsilon_{int})}{Q} e^{-E/k_BT} \tag{A3}$$

$$k_{cap} = k^\infty_{uni,r} K_{eq} \tag{A4}$$

$$K_{eq} = \frac{Q_{(AH^+ \cdot B)}}{Q_{AH^+} Q_B} e^{-\Delta H^\circ/kT} \tag{A5}$$

The partition function of the adduct $AH^+ \cdot B$ cancels out through eqs A3–A5 in calculating k_{cap}, and therefore k_{cap} is independent of the energy and frequencies assigned to the adduct. However, the rate through the central barrier does depend on these frequencies. This is because the frequencies assigned to the transition

(19) Forst, W. *Theory of Unimolecular Reactions*; Academic Press: New York, 1973.
(20) Wardlaw, D. M.; Marcus, R. A. *Adv. Chem. Phys.* **1987**, *70*, 231.

state for the forward reaction through the central barrier are identical with that in the adduct (except for the reaction coordinate).

The most novel feature of the present model for ion–molecule reactions is the use of competitive kinetics simultaneously through the loose, tight, and central complexes. Another novel feature is the microcanonical variational calculation of the capture rate through several loose complexes and the tight complex. This becomes significant for an accurate modeling of the transition from loose-complex-limited fast kinetics to tight-complex-limited slow kinetics.

The presence of the tight transition state leads to significant negative temperature coefficients of the capture rate. This is due to the low density of states in the tight transition state compared with the reactants and to the fact that the local potential at the position of the tight complex lies below the energy of the reactants. For similar reasons, the central barrier, with even smaller densities of states and lower potential energy can lead to even larger negative temperature coefficients and become rate limiting at higher temperatures.

Appendix II

Thermochemistry, Geometry, and RRKM Parameters. Energies, frequencies (cm^{-1}) and degeneracies, and rotational constants, symmetries, and dimensionalities of the various complexes and transition states in Figure 1 are needed for the RRKM models. Due to the lack of information about the ionic species and complexes, simplifying estimates are applied. In particular, all of the variations formed from frozen rotors are assigned a common frequency chosen such as to match the experimental or estimated entropy. The considerations applied to the various complexes will be described, followed by a list of the parameters applied to model several reaction systems.

a. Loose Complex. This complex develops at separations of r = 8–12 Å between the reactive NH^+ and N centers. When the loose complex is rate limiting, i.e., has the minimum flux, then $k_{pl} = k_{coll}$. The RRKM program examines several AH^+ to B separations to find the loose complex with the minimum flux.

In the loose complex, the reactants interact by weak ion–dipole and ion–induced dipole forces. For alkylpyridines, stereochemical calculations show that at $r > 9$ Å the reactants retain their free molecular rotations. Compared with the separated reactants, the entropies are decreased only by the change in translations and molecular rotations. For 2-$MePyrH^+$ + 2,6-t-Bu_2Pyr, this is calculated as −11.6 cal/(mol K) at 300 K and −13.6 cal/(mol K) at 500 K.

We examine loose complexes at r = 8, 10, 12, and 14 Å and select the one that minimizes the flux at any given internal energy E_{int} and rotational energy E_{rot}. The energies of the loose complexes are calculated from ion–dipole and ion–induced dipole formulas.[16] The rate constant is then calculated by integrating over E_{int} and E_{rot}.

b. Tight Complex. The second rate-limiting entity may develop at separations where the reactants interfere with the molecular and internal rotations of each other. This causes an adverse entropy effect, but the separation is too large for an effective compensating enthalpy effect.

Space-filling models and molecular computations[18] that rotate the reactants about the NH^+·N axis were constructed for the reactions of 2-$MePyrH^+$ + 2,6-t-Bu_2Pyr and 2,6-Et_2PyrH^+ + 2,6-t-Bu_2Pyr. The alkyl groups become locked and lose their internal rotations at $r(NH^+{\cdot}N)$ = 4–5 Å, where the angle available for rotation of the pyridine moieties decreases to 36° at 5 Å and 18° at 4 Å. We consider that in the latter the steric hindrance is nearly fully developed, the complex being somewhat less rigid than the hydrogen-bonded adduct.

As to the energy of the tight complex, calculations for NH^+·N bonds show that the bonding energy weakens by about 5 kcal/mol for stretching by 0.2 Å and by 4 kcal/mol for every 0.1 Å thereafter.[21-24] Therefore, if the N–N distance is stretched from the optimal 2.7 to 3.1–3.2 Å, the hydrogen bond is weakened to about 10–15 kcal/mol. Noting that E_{HB} = 25 kcal/mol and, from Figure 1, that the interaction energy in the tight complex is $E_{HB} - E_{tight}$, reasonable values for E_{tight} should be 10–15 kcal/mol. As for the entropies of the tight complexes, they may be more positive by 10–15 cal/(mol K) than those of the fully hydrogen-bonded adduct.

c. Hydrogen-Bonded Adduct and the Central Barrier. The complex where the NH^+·N hydrogen bond is optimized has the lowest energy but also the most negative entropy. We assume a similar geometry and thermochemistry at the central barrier, except a small added barrier to proton transfer.

The hydrogen-bonding energy for protonated pyridine complexes, whether unhindered or strongly hindered, is 25 ± 1 kcal/mol.[21] We shall use this value for E_{HB} (Figure 1). Ab initio calculations show a shallow surface for proton transfer between nitrogen centers, with barriers of 0–2 kcal/mol.[21-24] Jasinski and Brauman assigned 5 kcal/mol for thermoneutral proton transfer,[6] and for exothermic transfer the barrier should be lower. We use 2 kcal/mol for E_b.

The entropy of hydrogen-bonded complexes in the most hindered pyridine dimer measured in previous work, (2,6-i-$Pr_2Pyr)_2H^+$, is $\Delta S°$ = −45 cal/(mol K), refered to the separated reactants.[21] The severely hindered 2,6-t-Bu_2PyrH^+ shows $\Delta S°$ of −45 cal/(mol K) even in complexing with the small H_2O molecule.[9] In the present complexes with larger neutral partners, such as 2,6-Et_2PyrH^+ + 2,6-t-Bu_2Pyr, more internal rotors freeze and $\Delta S°$ should be at least −55 to −60 cal/(mol K), while 2-$MePyrH^+$ + 2,6-t-Bu_2Pyr has fewer hindered rotors and $\Delta S°$ is estimated as −45 to −55 cal/(mol K).

We estimate the vibrational frequencies of the various complexes as follows. We compose the frequencies of the alkylpyridines from those of pyridine[25] and the appropriate alkanes,[26] eliminating and adding characteristic C–H and C–C stretching and bending frequencies as needed. We also use our stereochemical program[18] to calculate the rotational moments of the loose and tight complexes, the two reactant moieties and the adduct, and the reduced moments of the internal rotors.

The space-filling models show that in the formation of the tight complex and adduct in 2-$MePyrH^+$ + 2,6-t-Bu_2Pyr 12 rotors are converted to torsions and in 2,6-Et_2PyrH^+ + 2,6-t-Bu_2Pyr 15 rotors are converted. In the absence of further knowledge, we use a common frequency for all the torsions. This frequency ν_{tight} and the energy of the tight complex E_{tight} are adjustable parameters. If the model is realistic, the values found for these parameters by fitting to experimental rate constants will yield a thermochemistry consistent with the estimates above. This is indeed found, as follows.

Figure 7 shows the RRKM results with a model for the highly hindered system 2,6-Et_2PyrH^+ + 2,6-t-Bu_2Pyr with parameters that fit the experimental kinetics. For the hydrogen-bonded central complex we use E_{HB} = 25 kcal/mol and E_b = 2 kcal/mol. We assign ν_b = 140 cm^{-1} to the 15 torsions formed from the rotors in the hydrogen-bonded adduct $(2,6\text{-}Et_2PyrH^+{\cdot}2,6\text{-}t\text{-}Bu_2Pyr)_{HB}$, corresponding to $\Delta S°(400)$ = −56 cal/mol for the formation of this adduct.

We then obtain the adjustable parameters for the tight complex from the best fit to the observed kinetics. The best fit is achieved with E_{tight} = 11.5 kcal/mol. In fact, the experimental line cannot be fitted with $E_{tight} < 8$ or $E_{tight} > 14$ kcal/mol with any value of ν_{tight}. Noting that the ion–neutral interaction energy in the tight complex is given by $E_{HB} - E_{tight}$ (Figure 1), the interaction energy is bracketed as 14 ± 3 kcal/mol. For the torsions the best fit yields ν_{tight} = 80 cm^{-1}, which gives $\Delta S°(400)$ = −40 cal/(mol K) for the

(21) Szczesniak, M. M.; Scheiner, S. J. Chem. Phys. 1982, 77, 4586.
(22) Scheiner, S.; Szczesniak, M. M.; Bigham, L. D. Int. J. Quantum Chem. 1983, 23, 739.
(23) Hillenbrand, E. A.; Scheiner, S. J. Am. Chem. Soc. 1984, 106, 6266.
(24) Scheiner, S. Acc. Chem. Res. 1985, 18, 174.
(25) Wilmshurst, J. K.; Bernstein, H. J. Can. J. Chem. 1957, 35, 1183.
(26) Pitzer, K. S.; Kilpatrick, J. E. Chem. Rev. 1946, 39, 435.
(27) Lias, S. G.; Liebman, J. F.; Levin, R. D. J. Phys. Chem. Ref. Data 1984, 13, 695.

tight complex with respect to the separated reactants. The results obtained for the adjustable parameters of $(2,6\text{-}Et_2PyrH^+ \cdot 2,6\text{-}t\text{-}Bu_2Pyr)_{tight}$ by fitting to the experimental rate constants are therefore consistent with the thermochemical estimates above.

Parameters for the $NH_4^+ + CH_3NH_2 \rightarrow CH_3NH_3^+ + NH_3$ Reaction. The energy and entropy of the hydrogen-bonded adduct $CH_3NH_3^+ \cdot NH_3$ with respect to the reactants has been determined as −21.4 kcal/mol and −26 cal/(mol K) at 400 K.[28] We shall assume similar thermochemistry for the adduct $NH_4^+ \cdot CH_3NH_2$. We assign a barrier, E_b, of 2 kcal/mol for proton transfer in the complex.

Space-filling geometric steric hindrance calculations[18] show that as the reactants approach, the steric angle by becomes restricted. The free angle decreases from 360° at an N–N distance of 5 Å to 49° at 3.5 Å. Accordingly, we chose 3–4 Å for the tight complex. The electrostatic interaction energy E_t at these distances is 5–10 kcal/mol, and we use values in this range. The parameters for the loose complexes are those of the separate reactants, except that the rotation of the dipole of CH_3NH_2 will be hindered due to the noncentral ion–dipole potential.

The experimental entropy change of −26 cal/(mol K) in forming the adduct is obtained by converting four molecular rotations of the reactants to torsions. The entropy of the tight complex should be less negative than that of the adduct, and the frequencies of the four torsions ν_{tight} are adjustable parameters.

Hydrogen-Bonded Adduct. Frequencies and degeneracies: 250, 5; 1000, 5; 1397, 3; 1450, 4; 1685, 2; 2960, 3; 3032, 1; 3134, 3; 3400, 2. (Frequencies of CH_3NH_2 are estimated from group frequencies. Vibrations at 250 cm^{-1} correspond to hindered molecular rotations of the reactants in the complex.) Rotational constants, symmetries, and dimensionalities: 3.62, 3, 1; 3.62, 3, 1; 0.7474, 1, 1. (CH_3 and NH_3 moments are treated as approximately equal). The last rotor is an active molecular rotation.

Transition State over Central Barrier for Proton Transfer. Frequencies and rotors are as above, but one 250-cm^{-1} vibration is transformed into a reaction coordinate. Barrier height above the adduct is 2 kcal/mol.

Tight Complex for Dissociation to Reactants. Frequencies are as above, except the 250-cm^{-1} vibrations are loosened to 150 cm^{-1}. NH_4^+ is removed from the optimal hydrogen-bonding distance to CH_3NH_3 but $H_3C\text{–}NH_2\text{–}H^+\text{–}NH_3$ retains tetrahedral geometry about the methylamine nitrogen. Rotational constants, symmetries, and dimensionalities: 3.63, 3, 1; 8.69, 3, 1; 0.86, 1, 1. (The second moment is the reduced moment for rotation about the stretched hydrogen bond.) The third rotor is an active molecular rotation. The energy of the tight complex above the adduct is 15 kcal/mol.

Loose Complex for Dissociation to Reactants. Frequencies are as above, but the 250-cm^{-1} vibrations are converted to free rotors. The internal rotors include the molecular rotations of the reactants. Rotational constants, symmetries, and dimensionalities: 3.62, 3, 1; 8.694, 3, 1; 0.6744, 1, 1; 5.43, 3, 2; 0.6912, 1, 2. The third rotor is an active molecular rotation of the overall complex. The last two rotors are active molecular rotations of the reactants within the complex. The rotational constant for inactive external (orbital) two-dimensional rotation depends on the separation of the reactants, with the separations (N–N distance) and constants as follows: 8 Å, 0.028 67; 10 Å, 0.017 98; 14 Å, 0.008 904; 18 Å, 0.005 292. Dissociation energy from the adduct is 22 kcal/mol.

Parameters for the Reaction of $2,6\text{-}Et_2PyrH^+$ with $2,6\text{-}t\text{-}Bu_2Pyr$. The frequencies are estimated from those of pyridine, ethane, and $i\text{-}C_4H_{10}$ by the addition and subtraction of C–H and C–C group frequencies as needed.

Hydrogen-Bonded Adduct. Frequencies and degeneracies: 140, 15; 371, 4; 374, 2; 405, 2; 437, 2; 450, 12; 605, 2; 652, 2; 675, 2; 703, 2; 749, 2; 799, 2; 886, 1; 921, 4; 942, 2; 965, 4; 981, 1; 992, 2; 1000, 3; 1029, 2; 1068, 3; 1098, 2; 1148, 2; 1172, 4; 1200, 2; 1217, 2; 1218, 1; 1300, 1; 1345, 4; 1375, 2; 1377, 4; 1439, 2; 1460, 12; 1482, 2; 1534, 2; 1572, 2; 1580, 2; 2950, 18; 3019, 4; 3046, 2; 3054, 4; 3083, 2. (Vibrations at 140 cm^{-1} correspond to 15 hindered rotors of the reactants in the complex.) Rotational constants, symmetries, and dimensionalities: 7.27, 3, 1; 7.27, 3, 1; 0.01215, 1, 1. The third rotor is an active molecular rotation.

Transition State over Central Barrier for Proton Transfer. Frequencies and rotors are as in the hydrogen-bonded adduct, but one 140-cm^{-1} rotor is converted into the reaction coordinate. Barrier height above the adduct is 2 kcal/mol.

Tight Complex for the Dissociation of the Adduct to Reactants. Ferquencies and rotors are as above, but 140-cm^{-1} vibrations are loosened to 80 cm^{-1}. Note that this is an adjustable parameter. The energy of the tight complex above the adduct is also an adjustable parameter, with a best fit to experiment at 11.5 kcal/mol.

Loose Complex for the Dissociation of the Adduct to Reactants. Frequencies area as above, but in the absence of frozen rotors, 140-cm^{-1} frequencies are absent. Rotational constants, symmetries, and dimensionalities: 10 alkyl rotors are represented for simplicity as 10 rotors of 7.27, 3, 1; 2 *tert*-butyl rotors of 0.273, 3, 1. Active free rotations of the reactants in the complex: 0.068 14, 1, 2; 0.1734, 1, 1; 0.012 98, 1, 2; 0.040 38, 2, 1. The third rotor is an active overall molecular rotation of the complex. the last two rotors are active rotations of the reactants within the complex. The rotational constant for the inactive external (orbital) two-dimensional rotation depends on the separation of the reactants, with the following separations (N–N distance) and constants: 8 Å, 0.002 88; 10 Å, 0.002 35; 12 Å, 0.001 502; 14 Å, 0.001 149. Dissociation energy from the adduct is 25 kcal/mol.

Parameters for the Reaction of the $2\text{-}MePyrH^+$ with $2,6\text{-}t\text{-}Bu_2Pyr$. The model is similar to the preceding system, with an adjustment for one methyl instead of two ethyl groups.

Registry No. 2-*t*-BuPyrH$^+$, 62907-59-9; 2,6-Et_2PyrH$^+$, 85048-76-6; 2-MePyrH$^+$, 16969-46-3; 2-*i*-PrPyrH$^+$, 76065-75-3; 2,6-Me_2Pyr-H$^+$, 17033-11-3; 2,6-*i*-Pr_2PyrH$^+$, 74570-68-6; Et_3NH^+, 17440-81-2; *n*-Pr_3NH^+, 50985-90-5; *n*-Bu_3N, 102-82-9; 2,6-*i*-Pr_2Pyr, 6832-21-9; 2,6-*t*-Bu_2Pyr, 585-48-8; *n*-Pr_3N, 102-69-2.

(28) Yamdagni, R.; Kebarle, P. *J. Am. Chem. Soc.* **1973**, *95*, 3504.